

AIAA 80-0042R

Plasma Collection by High-Voltage Spacecraft at Low Earth Orbit

I. Katz,* M. J. Mandell,† G. W. Schnuelle,‡
D. E. Parks,§ and P. G. Steen§
Systems, Science and Software, La Jolla, Calif.

A computer model of the three-dimensional sheath formation and plasma current collection by high-voltage spacecraft has been developed. By using new space charge density and plasma collection algorithms, it is practical to perform calculations for large, complex spacecraft. The model uses objects and geometries compatible with the NASA Charging Analyzer Program (NASCAP). Results indicate that ion focusing observed in the laboratory during high-voltage collection experiments is probably due to voltage gradients on the collecting surfaces.

Nomenclature

D	= renormalized screening length
e	= electron charge
I	= total collection current
j_0	= one-sided electron (ion) thermal current
k	= Boltzmann constant
L	= object dimension; computational mesh constant
\mathcal{L}_I	= variational function for ϕ_I
m	= electron (ion) mass
n_0	= ambient plasma density
r	= general space point
T	= renormalized plasma temperature
V	= particle velocity
V_0	= particle thermal velocity
x	= distance from sheath edge
δ	= functional derivative operator
ϵ_0	= permittivity of free space
θ	= plasma temperature
λ_D	= Debye (screening) length
ρ	= space charge density
ρ'	= derivative of space charge function with respect to potential
ϕ	= electrostatic potential
ϕ_I	= solution to I th linearized Poisson equation
ϕ_{IJ}	= j th iterate of solution for ϕ_I

Introduction

As satellite electrical power requirements increase, there is constant effort to increase operating voltages on solar arrays. The prime driver is weight reduction in both power cables and elimination of dc-to-dc converters used to supply high voltages to high-power microwave tubes or ion thrusters. One of the primary difficulties associated with high voltages on satellites in low Earth orbit is the power drain due to leakage currents flowing between exposed surfaces through the ambient plasma. The ground potential of an isolated object in space adjusts to collect no net plasma current. However, electrons collected by positive surfaces and positive ions collected by negative surfaces form current loops through the

plasma which waste solar array power. Early studies by Kennerud¹ have shown that small pinholes in insulation can make almost perfectly insulated solar arrays couple to an ambient plasma as effectively as bare metal plates. Thus, just covering exposed high voltages may not be an adequate solution.

In order to predict parasitic losses due to surrounding plasma, some simple models of plasma collection have been devised. These include models for current collection from other plasmas, such as ion engine efflux^{2,3} and simple models designed for low Earth orbit (LEO).^{4,5} Recently, large-scale experiments have been performed in the thermal vacuum test chamber at the NASA Johnson Space Center to simulate collection in LEO by a large (1 × 10-m) solar array.⁴

The purpose of this paper is to introduce a new three-dimensional computer model, NASCAP/LEO, which is designed to calculate plasma leakage currents. We will present the physical arguments that led to the model, followed by a brief description of the numerical techniques employed. We will then show results of applying this model to the NASA/JSC experiments of McCoy and Konradi.⁴ These simulations reproduced the observed ion focusing phenomenon; they are not intended to simulate the pinhole collection experiments of Kennerud.¹

Theory

We develop here a simplified nonlinear screening model for electric potentials and plasma structure surrounding an object with exposed high-voltage surfaces. We define high voltages ϕ by requiring that the potential energy associated with the voltage $e\phi$ be much larger than the plasma thermal energy θ

$$e\phi \gg k\theta$$

We also require that the Debye length λ_D of the plasma be less than, or at most comparable to, typical object dimensions L

$$\lambda_D < L$$

This clearly places us in the space charge limited collection regime. By utilizing these restrictions, we are able to reduce the Poisson-Vlasov equations which describe the plasma to a single nonlinear second-order differential equation.

In the limit of very small Debye length and very high voltages, a quasi-one-dimensional sheath forms in front of the collecting surface. The current in the sheath is the one-sided random thermal current

$$j_0 = n_0 e (k\theta / 2\pi m)^{1/2} \quad (1)$$

Presented as Paper 80-0042 at the AIAA 18th Aerospace Sciences Meeting, Pasadena, Calif., Jan. 14-16, 1980; submitted Jan. 18, 1980; revision received June 19, 1980. Copyright © American Institute of Aeronautics and Astronautics, Inc., 1980. All rights reserved.

*Program Manager.

†Research Scientist.

‡Senior Research Scientist.

§Junior Research Scientist.

The velocity within the sheath is

$$\frac{1}{2}mV^2 = \frac{1}{2}mV_0^2 + e\phi(r) \quad (2)$$

where

$$V_0 = (k\theta/2\pi m)^{1/2} \quad (3)$$

and the charge density is

$$\rho = -j_0/V \quad (4)$$

For $e\phi \gg k\theta$, this reduces to

$$\rho \rightarrow -n_0 e (k\theta/4\pi e\phi)^{1/2} \quad e\phi \gg k\theta \quad (5)$$

When the voltage drops down near the plasma potential, the charge density is determined by the exclusion of oppositely charged particles, and a Debye screening expression is valid:

$$\frac{\rho}{\epsilon_0} \rightarrow -\frac{\phi}{\lambda_D^2} \quad \lambda_D^2 = \frac{\epsilon_0 k\theta}{n_0 e^2} \quad e\phi < k\theta \quad (6)$$

Laframboise and Parker have shown that this expression is valid at very small potentials even for collisionless plasmas.⁶ Since the space charge limited potentials have an $x^{4/3}$ form, and the electric field has an $x^{1/2}$ dependence, then half the screening of the field is accomplished in the first one-eighth of the sheath. If object dimensions are large or comparable to sheath dimensions, then the one-dimensional charge density formulation can be used as an effective nonlinear screening to determine sheath potential contours.

Combining the low and high potential expressions, we can construct a single analytical formula which is a function of only the local potential and depends parametrically on the neutral plasma temperature and density

$$\frac{\rho(\phi)}{\epsilon_0} = -\frac{\phi}{\lambda_D^2} \left[1 + \sqrt{4\pi} \left(\frac{e\phi}{k\theta} \right)^{3/2} \right]^{-1} \quad (7)$$

This expression has the properties of going to the low potential Debye shielding limit [Eq. (6)] when $e\phi \ll k\theta$, and to Eq. (5) for $e\phi \gg k\theta$. The advantages of this expression over a particle tracking formulation for obtaining charge densities are overwhelming. Statistical and numerical difficulties preclude the direct approach for all but the very simplest problems. Using the screening formulation presented here reduces the complex Poisson-Vlasov sheath problem to a nonlinear equation, which for small potentials is Helmholtz in character:

$$\epsilon_0 \nabla^2 \phi + \rho(\phi) = 0 \quad (8)$$

We then use these potentials surrounding an object to define an approximate sheath boundary. Typically, we define the sheath to be the equipotential surface $\phi = k\theta/e$.

The sheath current density at the sheath boundary is the plasma thermal current. Thus, the total current collected is

$$I = \int_{\text{sheath boundary}} j_0 dS = j_0 \times \text{Area}_{\text{sheath}} \quad (9)$$

The distribution of currents on the spacecraft is found by the forward pushing of representative particles from the sheath boundary until they impinge upon the satellite. The particles start out with thermal velocity normal to the local sheath surface and are accelerated by the sheath electric fields. By integrating the product of the collected current and the local surface potential, the power drain can be computed.

The nonlinear screening model can be made more accurate by modifying the shielding due to focusing effects. The

particle tracking algorithms can calculate local enhancement of charge density due to the convergence of sheath particles. These terms can be used to modify the screening iteratively to reach a self-consistent solution. The final results would then be accurate for all ratios of object dimensions to sheath lengths.

Code Implementation

The implementation of the preceding ideas has been performed using the basic techniques developed for the standard NASA Charging Analyzer Program (NASCAP) code.⁷⁻⁹ Calculations proceed in four phases: 1) object definition, 2) solution of the nonlinear Poisson equation [Eq. (8)], 3) determination of the sheath boundary and its area, and 4) particle tracking to determine the current distribution on the test object.

Object Definition

Objects for NASCAP/LEO are defined using the standard NASCAP code. This takes advantage of the simple input and powerful graphics developed for the NASCAP. However, the preliminary version of NASCAP/LEO does not handle the full generality of the NASCAP-defined objects.

Nonlinear Potential Solution

The nonlinear Poisson equation [Eq. (8)] is solved iteratively by successive linearization (a multidimensional Newton-Raphson method). The linearized form of Eq. (8) is

$$-\epsilon_0 \nabla^2 \phi_I - \rho(\phi_{I-1}) - (\phi_I - \phi_{I-1})\rho'(\phi_{I-1}) = 0 \quad (10a)$$

or

$$-\epsilon_0 \nabla^2 \phi_I - \phi_I \rho'(\phi_{I-1}) = \rho(\phi_{I-1}) - \phi_{I-1} \rho'(\phi_{I-1}) \quad (10b)$$

where ρ' denotes $(\partial\rho/\partial\phi)$, and ϕ_I denotes the I th "major" iterate of the solution. The linear equation (10b) is solved iteratively (leading to a sequence of "minor" iterates ϕ_{Ij}) using (as in the NASCAP) a finite-element, scaled conjugate gradient method with provision for multiple nested grids with compatible boundary elements.

The finite-element formulation for Eq. (10b) is derived from the variational principle

$$\frac{\delta}{\delta\phi_I} \int d^3r \mathcal{L}_I(r) = 0 \quad (11a)$$

with

$$\begin{aligned} \mathcal{L}_I(r) = & (\epsilon_0/2) |\nabla\phi_I|^2 - \frac{1}{2}\rho'(\phi_{I-1})\phi_I^2 \\ & - \phi_I[\rho(\phi_{I-1}) - \phi_{I-1}\rho'(\phi_{I-1})] \end{aligned} \quad (11b)$$

Two points should be made concerning Eqs. (11). First, since Eq. (7) is non-monotonic, ρ' can be positive, leading to a non-positive-definite set of equations. We have found it satisfactory to circumvent this problem by making the replacement

$$\rho'(\phi_{I-1}) \rightarrow \max[0, \rho'(\phi_{I-1})] \quad (11c)$$

in Eq. (11b). Alternatively, a method¹⁰ designed to handle non-positive-definite problems might be adopted.

Second, if ρ' is too far negative so that the second term of Eq. (11b) dominates the first, the solution of Eqs. (11) is an unphysical oscillatory potential. This takes place for $\lambda_D < 0.7L$, where L is the local mesh spacing. These oscillations are eliminated by replacing Eq. (7) by a formula which has the same values for large ϕ , but no more screening than the code can resolve at small ϕ :

$$\rho(\phi)/\epsilon_0 = -(\phi/D^2) [1 + (\phi/T)^{3/2}]^{-1} \quad (12a)$$

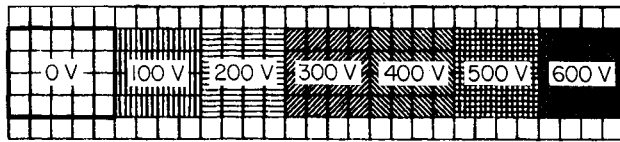


Fig. 1 Test object for sample calculations.

where

$$D = \max(\lambda_D, 0.7L) \quad (12b)$$

and

$$T = (k\theta/e)(4\pi)^{-1/2} (D/\lambda_D)^{4/3} \quad (12c)$$

For the typical case $T \gg k\theta/e$, the modified screening should be compensated for by defining the sheath boundary to be at some potential intermediate between θ and T .

For the sample calculations discussed in the following section, approximately 3-5 min of UNIVAC 1100/81 time were required for solution to Eq. (8).

Sheath Boundary Determination

The sheath boundary is determined by a set of routines which examine each finite element for the presence of a user-specified sheath boundary potential contour. The three-dimensional sheath contour is approximated in each selected element by a collection of contiguous triangles. The entire set of neighboring triangles defines the sheath boundary together with its area, and thus the net current collected.

Particle Tracking

Particle trajectories are followed by forward tracking from the centroid of each sheath boundary triangle. Each particle is given an initial current which is proportional to the local ambient flux and to the area of the triangle, an initial kinetic energy equal to a user-specified value, and an initial direction antiparallel to the local E -field (for electrons). The particle tracking is performed using Boris' second-order leapfrog scheme¹¹ with a dynamically adjustable time step. Provisions are included for magnetic field effects on particle motions. The actual particle tracking routines of NASCAP/LEO are straightforward adaptations of the NASCAP emitter particle tracking subroutines.

Sample Calculations

To illustrate the capabilities of NASCAP/LEO, we studied a system similar to one used in experiments by McCoy and Konradi.⁴ The system consisted of an object $8.7 \times 1.8 \times 0.3$ m with 1.2×1.2 -m patches which can be biased on one surface (Fig. 1). The labeled portions represent a conducting metal strip, while the border, sides, and back are insulating plastic. The biasing is indicated for case 4. The total area was 37.6 m^2 , and the metal area was 10.4 m^2 . It was modeled with 0.3 -m resolution in a volume $9.6 \times 9.6 \times 19.2$ m, filled with 2.3 -eV plasma with density $1.3 \times 10^6 \text{ cm}^{-3}$, and thus a debye length of 1 cm and a one-sided electron thermal current of 53 mA/m^2 .

All simulations were done in a positive bias (electron-collecting) mode. Similar results would be obtained for negative (ion-collecting) objects with currents reduced by the square root of the mass ratio. Seven test cases are shown here: 1) entire object at $+100$ V; 2) entire object at $+2400$ V; 3) plastic at ground, metal at $+2400$ V; 4) plastic at ground, metal biased as indicated in Fig. 1; 5) same as 4, but with potentials doubled ($V_{\max} = 1200$ V); 6) same as 4, but with potentials quadrupled ($V_{\max} = 2400$ V); and 7) same as 4, but with potentials octupled ($V_{\max} = 4800$ V).

The sheaths for cases 1 and 2 are illustrated in Fig. 2. For the 100 -V case, the sheath area was 69 m^2 , and for the 2400 -V

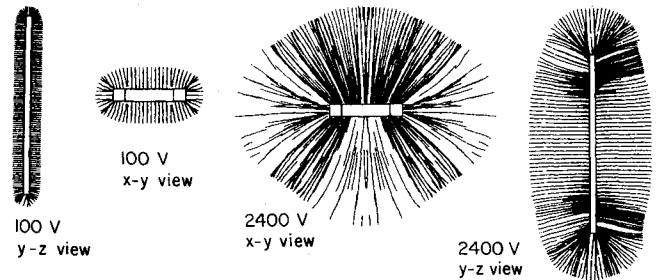


Fig. 2 Electron sheath particle trajectories for cases 1 and 2 with the test object at uniform potential.

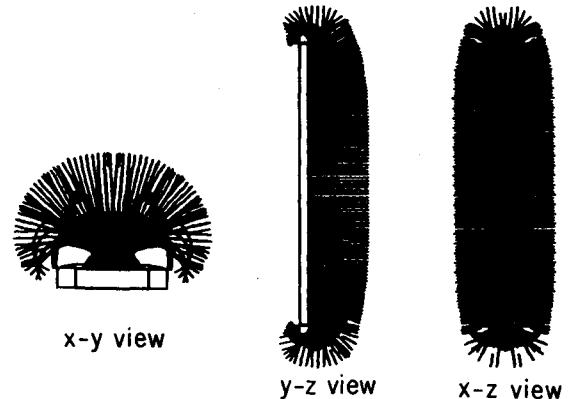


Fig. 3 Electron sheath particle trajectories for case 3.

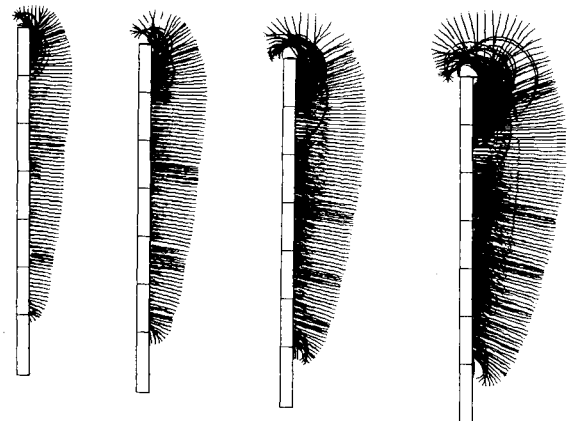


Fig. 4 y-z views of electron sheath particle trajectories for cases 4-7 (left to right).

case the sheath area was 258 m^2 , leading to collection currents of 3.66 and 13.7 A, respectively.

In the actual experiment, the object was not at uniform potential, but rather the insulating plastic collected sufficient current to remain near plasma ground. This was the motivation for cases 3-7, which provided more interesting potential contours and particle trajectories.

The sheath for case 3 is shown in Fig. 3. It is apparent that the sheath spills over the ends and sides to substantially enhance the current collection. The sheath area for this case was 92 m^2 , giving a current of 4.9 A. Note also the electrostatic focusing indicated by the x-y cross section of the particle trajectories, tending to concentrate the current near the center of the strip.

The sheaths for cases 4-7 are shown in Figs. 4 and 5. The sheath areas are 27 , 37 , 61 , and 81 m^2 , respectively. Electrostatic focusing effects similar to case 3 are observed. The current vs voltage is shown in Fig. 6. The cross indicates the mean current to a similar area of a panel whose conducting strip is uniformly held at 2400 V (case 3). Except for the high-

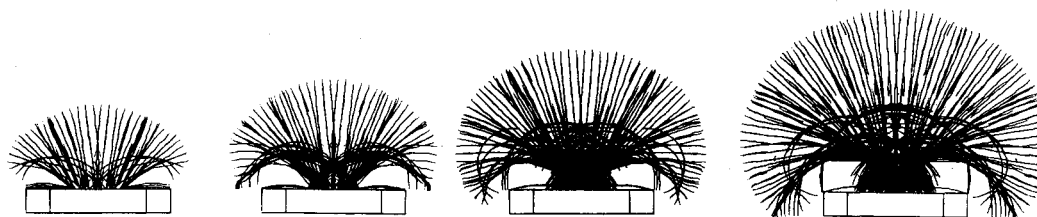


Fig. 5 x-y views of electron sheath particle trajectories for cases 4-7 (left to right).

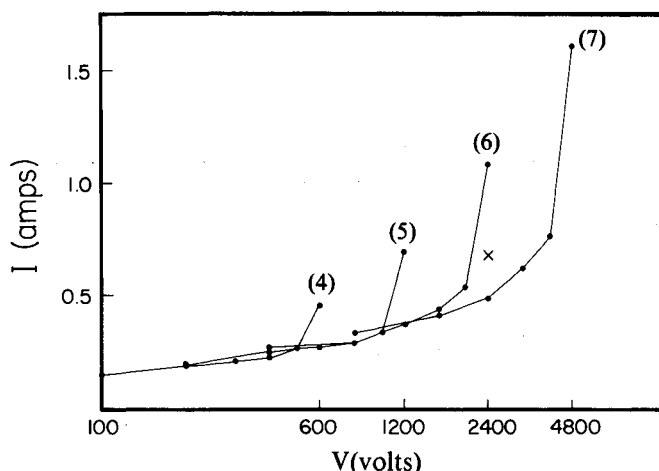


Fig. 6 Current per 1.44-m^2 section of panel vs potential for cases 4-7 (left to right).

voltage end of each panel, the points are not far from a universal curve, indicating that a two-dimensional representation would be fairly good in this case. Area enhancement factors range from ~ 2 at 100 V to ~ 10 at 3 kV. The greatly enhanced current to the end section of each panel is a three-dimensional effect and makes a substantial contribution to the power drain on the array.

A comparison of the results presented here with those of McCoy and Konradi must be approximate because the plasma in the experiment was far from homogeneous. The temperature and density we have chosen in our calculation correspond roughly to the estimate mean experimental values. The collection current per unit area from our calculation can be converted to argon ion current by dividing by the square root of the mass ratio, yielding a one-sided plasma current of 0.2 mA/m^2 . Then, for the 0-4800-V bias case, the predicted argon ion current collected per unit area is 1.6 mA/m^2 . This is quite close to the experimentally observed current of 2 mA/m^2 , far closer than one would expect due to the uncertainty in the experimental plasma parameters. That the calculation and experiment are in reasonable agreement, however, is certainly encouraging.

Summary

We have presented calculations using a preliminary version of NASCAP/LEO, a fully three-dimensional model for the

study of current collection by large high-voltage spacecraft. These calculations have reproduced both qualitative features such as ion focusing and quantitative ion collection currents observed in laboratory experiments. Extensions of NASCAP/LEO to include more complex geometries and materials as well as finer spatial resolution will increase the accuracy and applicability of the model. NASCAP/LEO should be a useful engineering tool for designing the spacecraft of the future.

Acknowledgments

This work was supported by NASA/Lewis Research Center, Cleveland, Ohio, and Air Force Geophysics Laboratory, Hanscom Air Force Base, Mass., under Contract NAS3-21762.

References

- ¹Kennerud, K.L., "High Voltage Solar Array Experiments," NASA CR-12180, 1974.
- ²Kaufman, H.R., "Interaction of a Solar Array with an Ion Thruster Due to the Charge-Exchange Plasma," NASA CR-135099, 1976.
- ³Parks, D.E. and Katz, I., "Spacecraft-Generated Plasma Interaction with High-Voltage Solar Array," *Journal of Spacecraft and Rockets*, Vol. 16, July-Aug. 1979, pp. 258-263.
- ⁴McCoy, J.E. and Konradi, A., "Sheath Effects Observed on a 10 Meter High Voltage Panel in Simulated Low Earth Orbit Plasma," *Spacecraft Charging Technology-1978*, NASA Conference Publication 2071, AFGL-TR-79-0082, 1979, p. 315.
- ⁵Parker, L.W., "Plasma Sheath Effects and Voltage Distributions of Large High-Power Satellite Solar Arrays," *Spacecraft Charging Technology-1978*, NASA Conference Publication 2071, AFGL-TR-79-0082, 1979, p. 341.
- ⁶Laframboise, J.G. and Parker, L.W., "Probe Design for Orbit Limited Current Collection," *Physics of Fluids*, Vol. 16, 1973, p. 629.
- ⁷Katz, I., et al., "A Three Dimensional Dynamic Study of Electrostatic Charging in Materials," NASA CR-135256, 1977.
- ⁸Katz, I., et al., "Extension, Validation and Application of the NASCAP Code," NASA CR-159595, 1979.
- ⁹Katz, I., et al., "The Capabilities of the NASA Charging Analyzer Program," *Spacecraft Charging Technology-1978*, NASA Conference Publication 2071, AFGL-TR-79-0082, 1979, p. 101.
- ¹⁰Luenberger, D.C., "Hyperbolic Pairs in the Method of Conjugate Gradients," *SIAM Journal of Applied Mathematics*, Vol. 17, 1969, p. 1263.
- ¹¹Boris, J.P., *Proceedings of 4th Conference on Numerical Simulation of Plasmas*, NRL, Washington, D.C., 1970, pp. 3-67.